Inorg. Chem. **2005**, *44*, 8756–8761

Synthesis and Structure of $Ta_4S_9Br_8$. An Emergent Family of Early Transition Metal Chalcogenide Clusters

Maxim N. Sokolov,*,† Artem L. Gushchin,† Pavel A. Abramov,† Alexandr V. Virovets,† Eugenia V. Peresypkina,† Svetlana G. Kozlova,†,‡ Boris A. Kolesov,† Cristian Vicent,# and Vladimir P. Fedin†

Nikolaev Institute of Inorganic Chemistry, Russian Academy of Sciences, pr. Lavrentyeva 3, Novosibirsk 630090, Boreskov Institute of Catalysis, Russian Academy of Sciences, pr. Lavrentyeva 5, 630090 Novosibirsk, Russia, and Departament de Ciencies Experimentals, Universitat Jaume I, Castellon, Spain

Received June 22, 2005

Single crystals of $Ta_4S_9Br_8$ are obtained by heating Ta, S, and Br_2 at 400 °C in a 4.0:9.0:4.0 molar ratio in a 44% yield. The structure was determined by X-ray analysis and consists of molecular clusters $[Ta_4(\mu_4\text{-}S)(\mu\text{-}S_2)_4Br_8]$. The tantalum atoms form a square with long Ta···Ta distances (3.30 Å), with four S_2 ligands bridging the Ta–Ta edges and one capping the square. Each Ta atom has two terminal bromine atoms. The compound is diamagnetic and has only two electrons for metal–metal bonding. IR and Raman spectral studies with the use of ^{34}S allow to identify characteristic vibrations S–S (537 cm^{-1}) and $Ta_4\text{-}\mu_4\text{-}S$ (407 cm^{-1}). The compound is soluble in CH_3CN, giving a dark-red solution with a characteristic electronic spectrum, which was assigned on the base of DFT calculations. ESI-MS spectra of the solutions show formation of $\{[Ta_4S_9Br_8]Br\}^-$ associates.

Introduction

Despite strong interest in the chemistry of sulfide clusters in general, sulfido-bridged cluster complexes of Ta remain little studied.[1] Self-assembly reactions in solution based on metathesis of mononuclear Ta(V) precursors with a sulfide source (generally, $(Me_3Si)_2S$) were used to prepare bi-, tri-, tetra-, and pentanuclear complexes without direct Ta−Ta bonding—mostly Cp derivatives and a thiotantalate, $[Ta_6S_{17}]$.[4−2,3] The only clusters with metal−metal bonding in this category are $[Ta_2S_2Cl_4(PR_3)_4]$ (a $Ta_2(\mu_2\text{-}S)_2^{4+}$ core) and a zigzag Ta_4 chain in $[Ta_4S_4Cl_8(PMe_3)_6]$.[4] High-temperature reactions lead to ternary sulfides and thiophosphates, where the $[Ta_2(S_2)_2]^{n+}$ ($n = 5, 6$) or $[Ta_2(S_2)(S)]^{6+}$ units are linked together by anionic ligands.[5] Ta−Ta bonding is observed in TaS_3 and Ta_6S_n ($n = 1, 3, 4$).[6] Reactions between Ta, S, and Br_2 or I_2 lead to chalcogen-poor trinuclear clusters $Ta_3(\mu_3\text{-}S)(\mu\text{-}X)_3^{7+}$ in the structures of Ta_3SBr_7 and $Ta_3SI_7\cdot TaI_4$, respectively.[7,8] We decided to explore high-temperature reactions between tantalum, chalcogen, and halogen in a chalcogen-richer area, with the hope to obtain ternary chalcohalides, where $Ta_xQ_y^{n+}$ cluster units would be coordinated by exchangeable halide ligands, thus permitting their further involvement into synthetic chemistry. Here we report the synthesis, structure determination, and detailed spectroscopic studies of a new tetranuclear Ta cluster, $[Ta_4(\mu_4\text{-}S)(\mu\text{-}S_2)_4Br_8]$.

Experimental Section

Materials and Spectroscopy. High-purity Ta and S powders were used. Br_2 was dried over P_4O_{10} and distilled. IR spectra (4000−40 cm^{-1}) were recorded on an IFS-85 Fourier spectrometer

* To whom correspondence should be addressed. E-mail: caesar@che.nsk.su.
† Nikolaev Institute of Inorganic Chemistry.
‡ Boreskov Institute of Catalysis.
# Universitat Jaume I.

(1) Sokolov, M. N.; Fedin, V. P. *Coord. Chem. Rev.* **2004**, *248*, 925.
(2) (a) Kawaguchi, H.; Tatsumi, K. *Organometallics* **1997**, *16*, 307. (b) Tatsumi, K.; Inoue, Y.; Kawaguchi, H.; Kohsaka, M.; Nakamura, A.; Cramer, R. E.; Van Coone, W.; Taogoshi, G. J.; Richmann, P. N. *Organometallics* **1993**, *12*, 352. (c) Fenske, D.; Maue, P. G. *Z. Naturforsch.* **1989**, *B44*, 531.
(3) Sola, J.; Do, Y.; Berg, J. M.; Holm, R. H. *Inorg. Chem.* **1985**, *24*, 1706.
(4) (a) Babaian-Kibala, E.; Cotton, F. A. *Inorg. Chim. Acta* **1991**, *182*, 77. (b) Babaian-Kibala, E.; Cotton, F. A.; Kibala, P. A. *Inorg. Chem.* **1990**, *29*, 4002.
(5) (a) Gutzmann, A.; Näther, C.; Bensch, W. *Inorg. Chem.* **2004**, *43*, 2998. (b) Evain, M.; Queignec, M.; Brec, R.; Rouxel, J. *J. Solid State Chem.* **1985**, *56*, 148. (c) Evain, M.; Queignec, M.; Brec, R.; Sourisseau, C. *J. Solid State Chem.* **1988**, *75*, 413.
(6) Rouxel, J. *Acc. Chem. Res.* **1992**, *25*, 328.
(7) Smith, M.; Miller, G. *J. Solid State Chem.* **1998**, *140*, 226.
(8) Smith, M.; Miller, G. *Inorg. Chem.* **2003**, *42*, 4165.

10.1021/ic051014e CCC: $30.25
Published on Web 10/19/2005

(Bruker) in KBr pellets. Raman spectra were obtained on a Triplimate SPEX spectrometer using a 632.8 nm line of He−Ne laser for excitation. UV/vis-spectroscopic measurements were conducted at room temperature using an Ultrospec 3300pro spectrometer. X-ray powder diffraction data were obtained on a DRON-2 powder diffractometer (Cu Kα radiation).

A Quattro LC (quadrupole−hexapole−quadrupole) mass spectrometer with an orthogonal Z-spray electrospray interface (Micromass, Manchester, UK) was used. The compound $Ta_4S_9Br_8$ was dissolved partially in acetonitrile by stirring thoroughly for 3 h. Sample solutions (approximately 10^{-4} M) were infused to the mass spectrometer via syringe pump directly to the interface at a flow rate of 10 μL/min. The temperature of the source block was set to 100 °C and the interface to 150 °C. A capillary voltage of 3.3 kV was used in the negative scan mode, and the cone voltage was kept at 20 V to avoid fragmentation of the pseudo-molecular ions. The drying gas, as well as nebulizing gas, was nitrogen at a flow of 400 and 80 L/h, respectively.

Cyclic voltammetry experiments were performed with a Echochemie Pgstat 20 electrochemical analyzer. All measurements were carried out with a conventional three-electrode configuration consisting of Pt working and auxiliary electrodes and a Ag/AgCl reference electrode filled with aqueous 3 M KCl. The solvent was CH_3CN (Merck isocratic grade). The supporting electrolyte was 0.1 M Bu_4NPF_6, prepared by reaction of tetrabutylammonium bromide and HPF_6, recrystallized from ethanol, and dried under vacuum. E_c values were determined at a scan rate of 100 mV/s.

Synthesis and Characterization. Ta powder (3.62 g, 0.020 mol), S (1.44 g, 0.045 mol), and Br_2 (3.20 g, 0.020 mol) were loaded in a quartz ampule, which was evacuated after three cycles of freezing/thawing by liquid N_2, flame sealed, and heated at 200 (1 day) and 400 °C (5 days) in a furnace with a small natural temperature gradient. Large single crystals of $Ta_4S_9Br_8$ deposit in the colder zone, together with some red-orange $TaBr_5$. Most of $Ta_4S_9Br_8$ remains in the hotter zone as pure single phase (powder diffraction). Yield of the product (collected from the hotter zone) 3.60 g (44%). Element ratio: $Ta_{4.0}$:$S_{9.1}$:$Br_{7.8}$ (EDAX). Raman (cm^{-1}): 537 m (S−S vibrations), 407 w (Ta_4-μ_4-S), 373 w, 365 w, 339 w, 292 s, 252 m, 229 s, 218 w, 197 w, 178 w, 163 w, 145 w, 125 sh, 119 s, 87 s, 75 w, 57 m. IR/FTIR (KBr disc/polyethylene): 538 m, 467 w, 408 w, 395 s, 337 m, 290 s, 269 m, 251 s, 232 vs, 226 vs, 218 vs, 168 w, 146 w, 125 w, 118 w, 106 s. Absorption spectrum (CH_3CN): λ_{max} (ϵ_M): 526 (1020), 750 (460) nm.

Cyclic voltammetry in the −1 to 1.2 V range displays two irreversible oxidations at 0.74 and 1.07 V and two irreversible reductions at −0.25 and −0.8 V, which most probably indicate a cluster degradation/fragmentation.

Structure Determination. The diffraction data were collected at room temperature on Bruker X8APEX CCD diffractometer with Mo Kα radiation ($\lambda = 0.71073$ Å) using φ scans of narrow (0.5°) frames. The structure was solved by direct methods and refined by the full-matrix least-squares method against $|F|^2$ in anisotropic approximation using the SHELXTL program set.[9] Absorption corrections were applied empirically using the SADABS program ($T_{min}/T_{max} = 0.510$).[10] The detailed data are collected in Table 1. Intermolecular interactions in crystals and topologies of molecular packing were analyzed with the program set for multi-purpose crystallochemical analysis TOPOS 4.0 Professional.[11] The KPACK program[12] was used to calculate packing coefficients and the following atomic radii: Ta, 1.43; S, 1.85; Se, 2.0; Br, 1.95; I, 2.15 Å.

Table 1. Crystal Data and Structure Refinement for $Ta_4S_9Br_8$[a]

chemical formula	$Br_8S_9Ta_4$
M_r	1651.62
cell setting, space group, Z	tetragonal, *I*4*mm*, 2
a (Å)	12.765 (5)
c (Å)	6.966 (4)
V (Å^3)	1135.0 (9)
D_x (mg m^{-3})	4.833
μ (mm^{-1})	34.11
crystal form, color	tetragonal prism, metallic black
crystal size (mm)	0.50 × 0.02 × 0.02
no. of measured, independent, and observed [$I > 2\sigma(I)$] reflns	2459, 656, 546
R_{int}	0.068
θ_{max} (°)	27.4
R1 [$F > 4\sigma(F)$], wR2 (F^2), GOF (F^2)	0.034, 0.070, 1.02
no. of reln/params	656/34
weighting scheme	calcd $w = 1/[\sigma^2(F_o^2) + (0.0183P)^2]$ where $P = (F_o^2 + 2F_c^2)/3$
$\Delta\rho_{max}$, $\Delta\rho_{min}$ (e Å^{-3})	1.59, −1.11

[a] Computer programs: APEX2 v.1.0-8 (Bruker, 2003); SHELXTL v.6.22 (Bruker, 1990−2003); local programs.

Theoretical Calculations. The electronic structure and vibrational spectra of the ground state of the isolated [$Ta_4S_9Br_8$] molecule (C_{4v} symmetry) was analyzed with the ADF 2002 program package.[13] The geometry optimization was achieved with the spin-restricted DFT, including zero-order scalar relativistic effects (ZORA[14]), in which model electron density functional Hamiltonians are represented as the sum of local density functionals LDA (VWN[15]) and gradient exchange functional GGA (Becke[16] and Perdew[17]). Slater orbitals (ADF/TZ2P) with core potentials Ta-(1s...5p), S(1s...2p), and Br(1s...3p) were used as basis wave functions. The formation energy corresponds to the process: 4Ta + 9S + 8Br → [$Ta_4S_9Br_8$]. Atomic charges were obtained by the Hirshfeld method.[18] Dipole-allowed electron transitions were calculated using the TDDFT (time-dependent density functional theory) method with the gradient exchange functional GGA LB94.[19]

Results and Discussion

Synthesis. The title compound is obtained by heating the elements in the required stoichiometric ratio at 400 °C. Some $TaBr_5$ also forms, together with an unidentified solid, which may be $TaOBr_2$, because its powder diffractogram resembles that of structurally characterized $TaOI_2$.[20] $Ta_4S_9Br_8$ is the second ternary compound obtained in the system Ta−S−Br_2. Trinuclear Ta(III) thiobromide, Ta_3SBr_7, is formed from the elements by heating the mixture at 550 °C in the

(9) *SHELXTL*, version 6.22; Bruker AXS, Inc.: Madison, WI, 2003.
(10) Sheldrick, G. M. *SADABS, Program for absorption correction with the SMART system*; University of Göttingen: Göttingen, Germany, 1996.
(11) Blatov, V. A.; Shevchenko, A. P.; Serezhkin, V. N. *J. Appl. Crystallogr*. **2000**, *33*, 1193; http://topos.ssu.samara.ru.
(12) Virovets, A. V.; Podberezskaya, N. V. *Kristallografiya* **1992**, *37*, 1017.
(13) *Amsterdam Density Functional (ADF) program*, release 2002.02; Vrije Universteit: Amsterdam, The Netherlands, 2002.
(14) Van Lenthe, E.; Ehlers, A. E.; Baerends, E. J. *J. Chem. Phys*. **1999**, *110*, 8943.
(15) Vosko, S. H.; Wilk, L.; Nusair, M. *Can. J. Phys*. **1980**, *58*, 1200.
(16) Becke, A. D. *Phys. Rev. A*. **1988**, *38*, 3098.
(17) Perdew, J. P. *Phys. Rev. B*. **1986**, *33*, 8822.
(18) Hirshfeld, F. L. *Theor. Chim. Acta* **1977**, *44*, 129.
(19) van Gisbergen, S. J. A.; Snijders, J. G.; Bearends, E. J. *J. Comput. Phys. Commun*. **1999**, *118*, 119.
(20) Ruck, M. *Acta Cryst. C* **1995**, *51*, 1960.

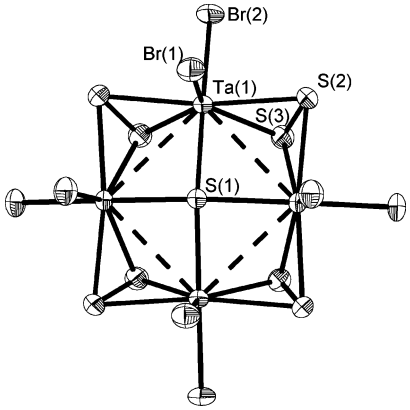

Figure 1. Structure of $Ta_4S_9Br_8$ (ellipsoids of 50% probability level).

stoichiometric ratio given by the formula.[7] The structural analogue of $Ta_4S_9Br_8$, the selenoiodide $Ta_4Se_9I_8$, was recently obtained from the elements.[21] However, the system Ta−Se−Br_2 under the same conditions forms $Ta_3Se_8Br_6$, which is built from positively charged patronite-like chains, $\cdots Ta(\mu\text{-}Se_2)_2\cdots$, separated by anions, $[TaBr_6]^-$.[22] The behavior of niobium, the closest analogue of tantalum, is very different. Instead of tetranuclear $Nb_4Q_9X_8$, which remains unknown, it generally forms dinuclear chalcohalides $[Nb_2(\mu\text{-}Q_2)_2X_4]$ or $[Nb_2(\mu\text{-}Q_2)(\mu\text{-}X)_2X_4]$.[23,24] As the mean oxidation state of the metal is +4.5 in the $Ta_4Q_9Br_8$ and +4 in $Nb_2Q_4X_4$ and $Nb_2Q_2X_6$, this different behavior may result from the higher electropositivity of Ta.

Crystal Structure. The molecule of $Ta_4S_9Br_8$ (**I**) is shown in Figure 1. The molecular structure is identical to that of $Ta_4Se_9I_8$ (**II**),[21] save that in **I** strict square planar geometry of the Ta_4 core is symmetrically imposed. Four S_2 ligands are asymmetrically coordinated to the Ta−Ta edges in a μ_2-η^2:η^2manner. Four of the sulfur atoms lie almost in the Ta_4 plane (within ±0.02 Å, equatorial, S_{eq}), and the other four (axial, S_{ax}) deviate from the plane by about 1.71 Å in the direction opposite to the μ_4-S atom. The terminal bromine atoms are also coordinated asymmetrically. Four of them lie closer to the Ta_4 plane (Br_{eq}, at 0.99 Å trans to the μ_4-S) and the rest deviate from this plane by 2.40 Å (cis to the μ_4-S). The interatomic distances and some angles are summarized in Table 2, and comparison of molecular geometry of **I** and **II** is given in Table 3. The coordination polyhedron around Ta can be described as pentagonal bipyramide with μ_4-S and one of the Br atoms trans to it in the axial position (Br_{trans}) and the two groups, S_2 and another Br atom (Br_{cis}), in the equatorial position. Rather long Ta−Ta distances (3.30 Å) are in agreement with the average Ta oxidation state of +4.5 in this highly electron-deficient cluster. In $[Ta(Se_2)_2]_2(TaBr_6)$ and $[Ta(Se_2)_2]_2I$, the distances between Ta atoms in the same average oxidation state are

Table 2. Bond Lengths [Å] and Angles [deg] for $Ta_4S_9Br_8$[a]

Ta(1)−S(1)	2.461(3)	S(2)−S(3)	2.061(8)
Ta(1)−S(2)	2.521(3)	Ta(1)−Br(1)	2.483(3)
Ta(1)−S(3)	2.500(4)	Ta(1)−Br(2)	2.471(2)
Ta(1)−Ta(1)[b]	3.3018(15)		
Ta(1)[b]−Ta(1)−Ta(1)[c]	90.0		
Ta(1)[c]−S(1)−Ta(1)	84.2(1)	S(1)−Ta(1)-Br(1)	86.1(2)
Br(2)−Ta(1)-Br(1)	99.1(1)	S(1)−Ta(1)-Br(2)	174.7(2)
S(1)−Ta(1)-S(3)	89.0(2)	Br(2)−Ta(1)-S(2)	86.5(9)
S(2)−Ta(1)-S(3)	48.5(2)	Br(1)−Ta(1)-S(2)	88.5(2)
S(1)−Ta(1)-S(2)	93.7(8)	Br(1)−Ta(1)-S(3)	136.2(1)
S(3)−Ta(1)-S(3)[b]	87.0(2)	Br(2)−Ta(1)-S(3)	87.1(1)
S(2)[b]−Ta(1)−S(2)	171.8(1)		

[a] Symmetry transformations used to generate equivalent atoms: b, $-y$, x, z; c, y, $-x$, z; d, $-x$, $-y$, z.

Table 3. Average Molecular Geometry of $Ta_4Q_9X_8$

		deviation of the atoms from Ta_4 plane, Å					
compound	Ta···Ta, Å	Ta	Q_{eq}	Q_{ax}	μ_3-Q	X_{eq}	X_{ax}
$Ta_4S_9Br_8$ (**I**), Q = S, X = Br	3.301	0	−0.02	1.71	−0.78	0.99	−2.40
$Ta_4Se_9I_8$ (**II**), Q = Se, X = I	3.392	±0.006	−0.13	1.86	−1.02	0.93	−2.65

3.18−3.23 and 3.20 Å, respectively.[22,25] This is expectedly longer than in the clusters with Ta−Ta bond of order 1, such as $Ta^{III}_3SBr_7$ (2.86 Å) or in $[Ta_2(\mu\text{-}S)_2Cl_4(PMe_2Ph)_4]$ (2.875 Å).[4] The situation with no Ta−Ta bonding is found in $Ta^{V}_2(\mu\text{-}S_2)_2^{6+}$, present in $TaPS_6$ and $Ta_4P_4S_{29}$.[5b] In this case Ta···Ta distances are 3.36−3.38 Å, i.e., somewhat longer than in **I**, which has two electrons to provide a weak bonding between Ta atoms, as supported by DFT calculations (vide infra). The S−S distances correspond to a single bond, as expected for the S_2^{2-} formalism.[26] The Ta−Br bond lengths are practically the same as those found in the $[TaBr_6]^-$ salts.[22]

There are other square planar clusters with capping μ_4-S, $[Nb_4(\mu_4\text{-}S)_2(\mu\text{-}SPh)_8(SPh)_4]^{4-}$ and $[Nb_4(\mu_4\text{-}S)_2(\mu\text{-}SPh)_8(PMe_2R)_4]$,[27] but no Ta analogues are known. A μ_4-STa_4 unit is found in $[Cp_4Ta_4(S_2)_5(\mu_4\text{-}S)(\mu\text{-}S)_2]$. In that case, the μ_4-S ligand is found in the center of a Ta_4 tetrahedron, with very long Ta−S distances (2.62−2.67 Å).[2c] On the other hand, in the triangular cluster $[Ta_3(\mu_3\text{-}S)(\mu\text{-}Br)_3Br_4]$, the Ta-capping μ_3-S distances (2.36−2.44 Å) are even shorter than in **I**, which reflects the increasing electron deficiency of the capping μ_4-SM_4 bonding vs μ_3-SM_3: in both cases, the capping sulfur donates only four electrons.[7]

Despite similar molecular geometries, the intermolecular interactions in the crystals of **I** and are different. In **II,** four shortened nonvalent contacts $Se_{ax}\cdots I$ (3.484(1)−3.581(1) Å) are all directed to the same iodine atom so that the molecules are joined into zigzag chains (Figure 2a). In **I** (Figure 2b), relatively short $S_{ax}\cdots Br$ contacts are arranged in a quite different way, forming a crownlike system of eight symmetrically equivalent contacts of 3.558(5) Å. Each S_{ax} atom forms two contacts with a pair of bromine atoms (3.550(5)

(21) Sokolov, M. N.; Gushchin, A. L.; Virovets, A. V.; Peresypkina, E. V.; Kozlova, S. G.; Fedin, V. P. *Inorg. Chem.* **2004**, *43*, 7966.
(22) Sokolov, M.; Imoto, H.; Saito, T.; Fedorov V. *Polyhedron* **1998**, *17*, 3735.
(23) (a) Rijnsdorp, J.; DeLonge G. L.; Wiegers, G. A. *J. Solid State Chem.* **1979**, *30*, 365. (b) von Schnering, H. G.; Beckmann, W. *Z. Anorg. Allg. Chem.* **1966**, *347*, 231.
(24) Franzen, H. F.; Hönle, W.; v. Schnering, H. G. Z. *Anorg. Allg. Chem.* **1983**, *497*, 13.
(25) Gressier, P.; Guemas, L.; Meerchaut, A. *Acta Crystallogr. B* **1982**, *38*, 2877.
(26) Müller, A.; Jaegermann, W.; Enemark, J. H. *Coord. Chem. Rev.* **1982**, *46*, 245.
(27) (a) Seela, J. L.; Huffmann, J. C.; Christou, G. *J. Chem. Soc. Chem. Commun.* **1987**, 1258. (b) Babaian-Kibala, E.; Cotton, F. A.; Kibala, P. A. *Polyhedron* **1990**, *9*, 1689.

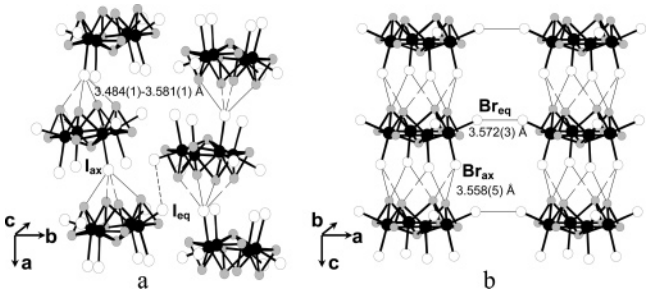

Figure 2. Comparison of crystal structures of $Ta_4Se_9I_8$ (a) and $Ta_4S_9Br_8$ (b). The short interatomic $Q\cdots X_{ax}$ and $X_{eq}\cdots X_{eq}$ contacts are shown as dashed lines. (a) The antiparallel chains of $Ta_4Se_9I_8$ molecules in the crystal packing of **II**. The chains are joined to the 3D framework by I···I 3.948(1) and 4.040(1) Å contacts. (b) The parallel chains of $Ta_4S_9Br_8$ molecules in the crystal packing of **I**. The chains are joined to the 3D framework by short $Br_{eq}\cdots Br_{eq}$ contacts.

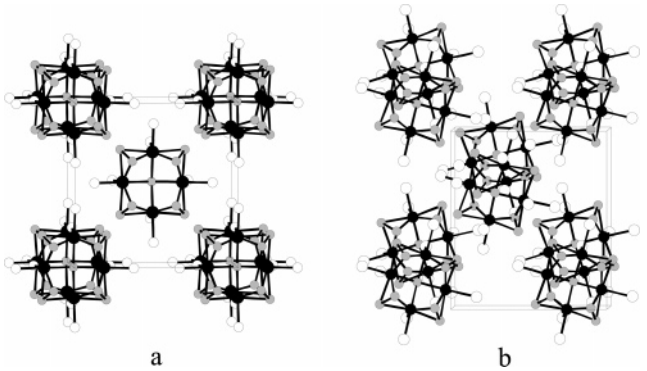

Figure 3. Crystal paking (a) in **I** (view along [001]) and (b) in **II** (view along [100]).

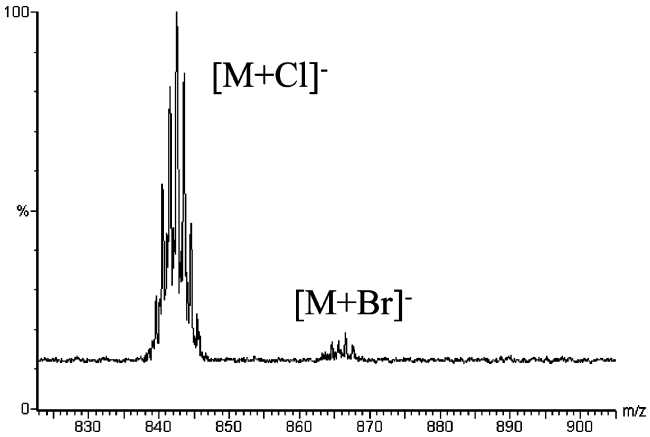

Figure 4. ESI mass spectrum of $Ta_4S_9Br_8$ in CH_3CN in the presence of 1 equiv of PPh_4Cl in the negative scan mode.

Å), thus involving all axial bromine atoms of the adjacent molecule into intermolecular bonding. As in **II**, the $Q_{ax}\cdots X$ contacts join molecules into chains, but the chains in **I** are strictly linear and run in the same direction, resulting in a polar structure. Shortened intercontacts $Br_{eq}\cdots Br_{eq}$ (3.572(3) Å) join the chains into a 3D framework. The different way of intermolecular bonding in these two structures leads to different arrangements in the first coordination sphere of the molecules. Each molecule in crystal of **I** is surrounded by 14 neighbors, while in **II**, they are only surrounded by 8 (Figure 3). In both structures, two of the closest molecules are the adjacent molecules of the chain. The distance between

Table 4. Calculated and Experimental Geometry of $Ta_4S_9Br_8$

d(Ta−Ta), Å		d(Ta−S), Å		d(Ta−μ_4-S), Å		d(Ta−Br), Å		d(S−S), Å	
calcd	exptl	calcd	exptl	calcd	exptl	calcd	exptl	calcd	exptl
3.346	3.301	2.533 2.551	2.500 2.521	2.497	2.461	2.509 2.521	2.471 2.483	2.198	2.061

Table 5. Calculated Atomic Charges in $Ta_4S_9Br_8$

Ta	S	μ_4-S	Br
0.245	0.009 (ax) 0.024 (eq)	−0.104	−0.121 (cis) −0.131 (trans)

their centers of gravity in **I** is of 6.966 Å, in **II**, the distance is 7.744 Å.

Both **I** and **II** show a very strong structural similarity to the recently prepared Ln(III)−Se clusters $[Ln_4(\mu_4\text{-Se})(\mu\text{-Se}_2)_4(THF)_6I_2]$ (Ln = Tm, Ho, Er, Yb).[28] The molecular Ti thiochloride $[Ti_4(\mu_4\text{-O})(\mu\text{-S}_2)_2(\mu\text{-Cl})_2Cl_4]$ has a similar structure, with the difference that the coordination requirements of Ti atoms are satisfied with a lower Cl/Ti ratio by making two Cl ligands to bridge two opposite Ti atoms; the Ti_4 arrangement is in fact a flattened tetrahedron.[29] In a broader sense, both **I** and the Ln clusters can be regarded as higher homologues of $M_3(\mu_3\text{-Q})(\mu,\eta^2\text{-Q}_2)_3$ (M = Ti, V, Mo, W, Re; Q = O, S, Se, Te) clusters with three metal atoms and three bridging dichalcogen ligands instead of four in our case.[30] In both cluster types, the μ_2-Q_2 ligands are tilted to the M_n (n = 3, 4) plane, permitting the distinction to be made between axial and equatorial chalcogen atoms. The $M-Q_{eq}$ bond distances are sufficiently longer than $M-Q_{ax}$ (sometimes by up to 0.1 Å), though this difference is less pronounced in the square clusters, probably due to the elongation of metal−chalcogen bonds. In **I**, the difference is only 0.02 Å. Each M atom both in M_4Q_9 and in M_3Q_7 cores coordinates two terminal atoms. The Q−Q bonds remain almost unchanged. Moreover, just like **I** and **II**, the crystal structures of M_3Q_7 clusters contain a negatively charged atom or ion nearly equidistant from three Q_{ax} atoms, with short nonbonding contacts between them.[31] The contacts are much shorter then the sum of van der Waals radii. Thus,

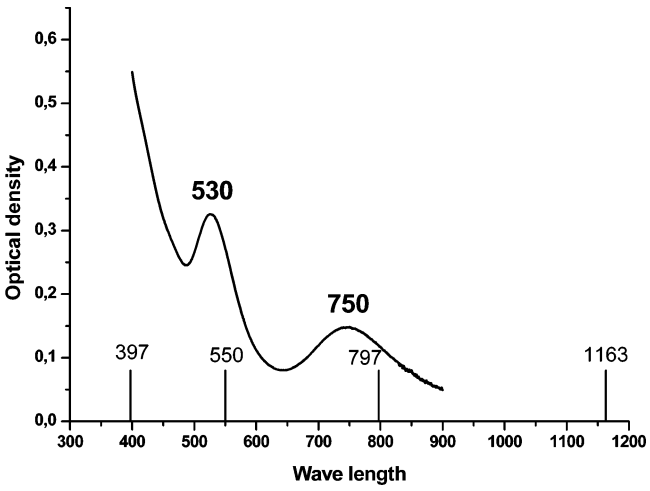

Figure 5. Experimental and calculated (vertical lines) electronic spectrum of $Ta_4S_9Br_8$ in CH_3CN.

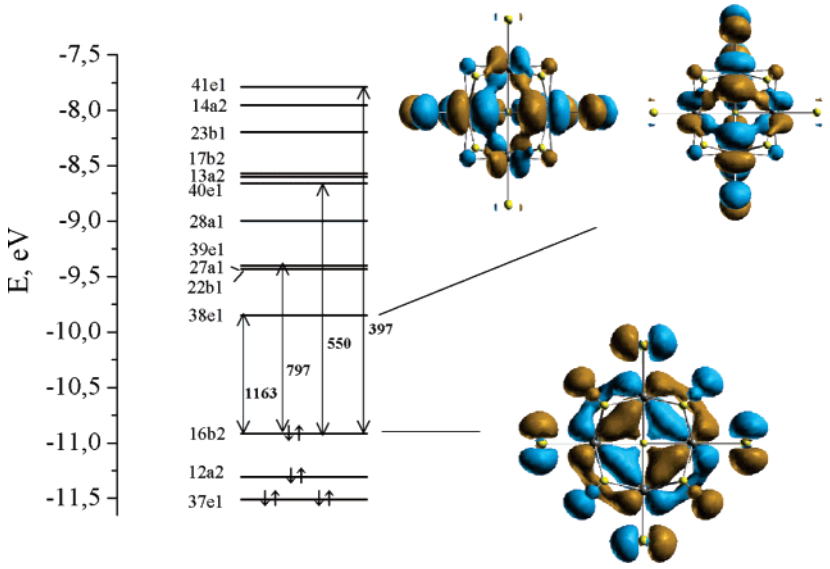

Figure 6. The energy level diagram and schematic figures of MO calculated at the DFT level with GGA LB94 and allowed electron transitions (arrows) in the $Ta_4S_9Br_8$ molecule.

the bridging Q_2^{2-} group in $[Ta_4(\mu_4\text{-}Q)(\mu,\eta^2\text{-}Q_2)_4X_8]$ has similar electrophilic character as Q_2^{2-} in the M_3Q_7 clusters.

Mass Spectrometry. In the ESI-MS of **I** (CH_3CN solution, negative scan mode), only one peak is observed, which is attributed to the formation of ionic associate $\{[Ta_4S_9Br_8]Br\}^-$, most probably via the four $S_{ax}\cdots X^-$ interactions. Despite the neutral nature of complex $Ta_4S_9Br_8$, it readily ionizes in the negative scan mode by capturing a bromide. The intensity of the signal increases when some Bu_4NBr is added. With Ph_4PCl (1 equiv), the formation of $\{[Ta_4S_9Br_8]Cl\}^-$(or, less probably, $\{[Ta_4S_9Br_7Cl]Br\}^-$) is observed (Figure 4). This ionization mode is unusual as compared with other neutral halide metal complexes reported by Henderson et al.[32] In these complexes, the loss of one halide ligand appears to be the dominant ionization process, though aggregation with cationic species also was detected in some cases. Positive ESI mass spectra of $Ta_4S_9Br_8$ show no signals of any cluster species present in the gas phase. The lack of the ionization through a halide loss process might be attributed to the high stability of the Ta−Br bonds in the compound. There are close parallels with trinuclear clusters $[Mo_3S_7X_6]^{2-}$, which tend form anionic associates $\{[Mo_3S_7X_6]X\}^{3-}$, also via $S_{ax}\cdots X^-$ contacts (X = Cl, Br).[33]

Electronic Structure and UV−Vis Spectra. According to the calculations, the formation of $Ta_4S_9Br_8$ molecule is a highly exothermic process (−101.0 eV). The optimized structure parameters are given in Table 4. There is a qualitative agreement between the calculated and experimental data. The difference is to be explained by the inevitable discrepancies between the values obtained for an isolated molecule in a vacuum and the real fragment of the crystal lattice. Table 5 shows the calculated atomic charges. The Ta and S atoms are slightly positively charged, whereas the μ_4-S and Br atoms bear small negatively charges. However, the small absolute values confirm the essentially covalent bonding in the molecule. The HOMO is a nondegenerate orbital $16b_2$, has ∼50% contribution of 5d Ta AO, ∼20% from 3p S AO (from S_{eq}), and another ∼20% from 4p Br AO with bonding character for $Ta-S_{eq}$ and antibonding character for $Ta-Br_{trans}$ (Figure 6). The calculated ground state of the $Ta_4S_9Br_8$ molecule is spin-paired (diamagnetic) and correlates well with the experimental data. Only two electrons are thus available for metal−metal bonding, which gives the bond order between each pair of Ta atoms as 0.25, in accordance with the observed elongated Ta−Ta distance. The LUMO is a double degenerate orbital $38e_1$, has a mixture of bonding and antibonding character with ∼60% contribution of 5d Ta AO, ∼5% of 3p S AO (3.5% from μ_4-S ligand), and ∼20% of 4p Br AO (Figure 6).

To assign the bands in the electronic spectrum, it was assumed that they correspond to the electron-dipole transitions from HOMO to the LUMO and higher orbitals. For the C_{4v} symmetry, the selection rules allow $b_2 \leftrightarrow e$ transitions. In the window available for study, these are $16b_2 \leftrightarrow 38e_1$, $16b_2 \leftrightarrow 39e_1$, $16b_2 \leftrightarrow 40e_1$, and $16b_2 \leftrightarrow 41e_1$ transitions (Figures 5 and 6). The TDDFT predicts almost equal intensities for all four transitions. However, the experimental data demonstrate that the intensity is higher at lower

(28) (a) Kornienko, A.; Melman, J. H.; Hall, G.; Emge, T. J.; Brennan, J. C. *Inorg. Chem.* **2002**, *41*, 121. (b) Fitzgerald, M.; Emge, T. J.; Brennan, J. G. *Inorg. Chem.* **2002**, *41*, 3528. (c) Melman, J. H.; Fitzgerald, M.; Freedman, D.; Emge, T. J.; Brennan, J. G. *J. Am. Chem. Soc.* **1999**, *121*, 10247.

(29) Cotton, F. A.; Feng, X.; Kibala, P.; Sandor, R. B. W. *J. Am. Chem. Soc.* **1989**, *111*, 2148.

(30) (a) Sokolov, M. N.; Fedin, V. P.; Sykes, A. G. *Compr. Coord. Chem. II* **2003**, *4*, 761. (b) Saito, T. J. *Chem. Soc., Dalton Trans.* **1999**, 97. (c) Beck, J.; Müller-Buschbaum, K. *Z. Anorg. Allg. Chem.* **1999**, *625*, 1212.

(31) Mayor-Lopez, M. J.; Weber, J.; Hegetschweiler, K.; Meyenberger, M. D.; Jobo, F.; Leoni, S.; Nesper, R.; Reiss, G.; Frank, W.; Kolesov, B.; Fedin, V.; Fedorov, V. *Inorg. Chem.* **1998**, *37*, 2633.

(32) Henderson, W.; Evans, C. *Inorg. Chim. Acta*, **1999**, *294*, 183.

(33) (a) Lu, S.; Shang, M.; Huang, J. *Chin. J. Struct. Chem. (Jiegou Huaxue)* **1984**, *3*, 9. (b) Huang, J.; Shang, M.; Huang, J.; Zhuang, H.; Lu, S.; Lu, J. *Chin. J. Struct. Chem. (Jiegou Huaxue)* **1982**, *1*, 1. (c) Klingelhöfer, P.; Müller, U.; Friebel, C.; Pebler, J. *Z. Anorg. Allg. Chem.* **1986**, *543*, 22. (d) Fedorov, V. E.; Gerasko, O. A.; Mironov, Yu. V.; Hegetschweiler, K.; Stoop, R.; Gallus, J.; Gramlich, F. *Russ. J. Struct. Chem., Engl. Transl.* **1995**, *36*, 956.

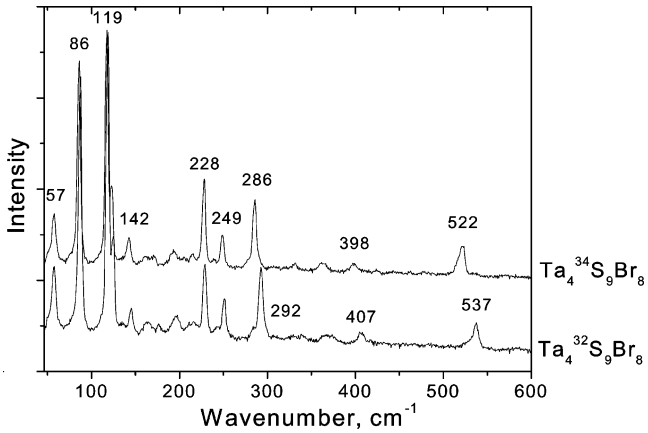

Figure 7. Raman spectra of the isotopomeric $Ta_4{}^{32}S_9Br_8$ and $Ta_4{}^{34}S_9Br_8$.

Table 6. Isotopic Shifts in the Raman Spectra of $Ta_4S_9Br_8$

ω (^{32}S)	ω (^{34}S)	$\Delta\omega$	ω (^{32}S)	ω (^{34}S)	$\Delta\omega$
57	57	0	216	215	1
87	86	1	229	228	1
119	117	2	243	240	3
125	123	2	251	249	2
145	143	2	292	286	6
163	161	2	407	398	8
176	171	5	537	522	15
196	194	2			

wavelengths and that HOMO−LUMO bands cannot be observed. We suppose that this is due to the vibronic effects when the electrons are excited into degenerate e_1 levels.[34]

Vibration Spectra. For C_{4v} $Ta_4S_9Br_8$, the internal vibrations are represented as $\Gamma = 10A_1$ (Raman, IR) + $4A_2$ + $6A_1$ (Raman) + $7A_2$ (Raman) + 14E (Raman, IR). The experimental Raman spectra for $Ta_4{}^{32}S_9Br_8$ and $Ta_4{}^{34}S_9Br_8$ isotopomeric molecules are shown in Figure 7. The Raman isotopic shifts upon $^{32}S \rightarrow {}^{34}S$ substitution are given in Table 6. It can be seen that most of the vibration modes undergo some isotopic shift, but the most sensitive are the bands at 292, 407, 537 cm^{-1} and a very weak band at 176 cm^{-1}. The numerical values for the isotopic shifts in the IR spectra together with the normal coordinates can be found in the Supporting Information. The characteristic band at 537-(Raman)/538(IR) cm^{-1} is due to the ν(S−S) vibration in the bridging S_2, and a weak doubly degenerate mode 407-(Raman)/408(IR) cm^{-1} comes from Ta−μ_4-S vibrations. The band at 292(Raman)/292(IR) cm^{-1} corresponds to Ta−μ_2-S_2. For the other vibrations, the calculated eigenvectors are complex and include the participation of all the atoms in each of them.

The position of ν(S−S) at 537(Raman)/538(IR) cm^{-1} in **I** correlates well with the positions of this vibration in other studied S_2 complexes with the same disulfide bridging mode—in $[W_2(\mu\text{-}S_2)_2Br_8]^{2-}$ (590(IR)/592(Raman) cm^{-1}); $[Mo_2(\mu\text{-}S_2)_2Br_8]^{2-}$ (598(IR)/601(Raman) cm^{-1}); $[Mo_3(\mu_3\text{-}S)(\mu\text{-}S_2)_3Cl_6]^{2-}$ (560(IR)/568(Raman) cm^{-1}); $[W_3(\mu_3\text{-}S)(\mu\text{-}S_2)_3Br_6]^{2-}$ (550(IR)/560(Raman) cm^{-1});[35] and $[Nb_2(\mu\text{-}S_2)_2Br_8]^{2-}$ (576 cm^{-1}, IR).[36] The characteristic M−μ_3-S vibrations are observed at 461 cm^{-1} in $[Mo_3(\mu_3\text{-}S)(\mu\text{-}S_2)_3Cl_6]^{2-}$ and at 449 cm^{-1} in $[W_3(\mu_3\text{-}S)(\mu\text{-}S_2)_3Br_6]^{2-}$ (Raman, IR), that is, higher than the Ta−μ_4-S vibration in **I**.

Acknowledgment. Grants to M.N.S. of Russian Science Support is gratefully acknowledged. The work was supported by INTAS (Grant No. 2356), Russian Science Support Foundation for Basic Research (grant 05-03-32126) and Haldor Topsøe foundation (a grant for A.L.G.). The authors thank Prof. V. A. Blatov for providing TOPOS 4.0 Professional software.

Supporting Information Available: Crystallographic information file (CIF) for **I**. This material is available free of charge via the Internet at http://pubs.acs.org. The details of the theoretical IR and Raman spectra calculations are available from the authors upon request.

IC051014E

(34) Bersuker, I. B. *Electronic Sructure and Poperties of Transition Metal Compounds*; Jonh Wiley and Sons: New York, 1996. Bersuker, I. B. *The Jahn−Teller Effect and Vibronic Interactions in Modern Chemistry*; Plenum Press: New York, 1984.

(35) (a) Fedin, V. P.; Kolesov, B. A.; Mironov, Yu. V.; Gerasko, O. A.; Fedorov, V. Ye. *Polyhedron* **1991**, *10*, 997. (b) Fedin, V. P.; Sokolov, M. N.; Gerasko, O. A.; Kolesov, B. A.; Fedorov, V. Ye.; Mironov, A. V.; Yufit, D. S.; Slovohotov, Yu. L.; Struchkov, Yu. T. *Inorg. Chim. Acta* **1990**, *175*, 217. (c) Fedin, V. P.; Sokolov, M. N.; Mironov, Yu. V.; Kolesov, B. A.; Tkachev, S. V.; Fedorov, V. Ye. *Inorg. Chim. Acta* **1990**, *167*, 39.

(36) Sokolov, M.; Imoto, H.; Saito, T.; Fedorov, V. *Z. Anorg. Allg. Chem.* **1999**, *625*, 989.